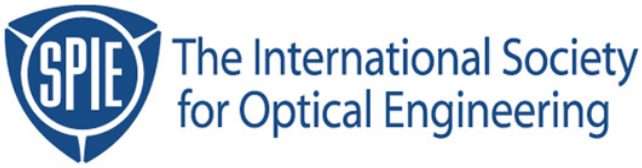

This paper was published in the proceedings of
Optical Microlithography XIV, SPIE Vol. 4346, pp. 1522-1532.
It is made available as an electronic reprint with permission of SPIE.

Impact of Illumination Coherence and Polarization on the Imaging of Attenuated Phase Shift Masks

Z. Mark Ma
Texas Instruments, 1357 N. Central Expressway, Dallas, TX 75243
Chris A. Mack
KLA-Tencor, 8834 N. Capital of Texas Hwy, Suite 301, Austin, TX 78759

Abstract

Attenuated phase shift masks (PSM) have been widely used in photolithography to enhance resolution and process margin. The advantage of attenuated PSM is further enhanced when it is combined with off-axis illumination (OAI) and optical proximity correction (OPC). This combination results in better performance than when attenuated PSM or OAI is used separately. However, the performance of isolated features is still a limiting factor to improve process margin. One result of such resolution enhancement techniques in conjunction with high numerical aperture imaging systems is an increase in the angles of the light used to form the images. Polarization mismatching among interacting beams becomes worse as the incident angle increases. In this paper we use contact hole patterning as an example to demonstrate how polarization plays a role with different partial coherence factors. PROLITH/3D simulation was used to compare and explain experimental results.

Keywords: Optical lithography simulation, polarization, PROLITH

Introduction

Phase shift mask (PSM) technology has been widely used in photolithography to enhance resolution and process margin. The application of PSM will be extended further as design rules continuously shrink to smaller than the exposure wavelength. Among the variety of phase shift technologies, attenuated PSM (attPSM) is the most commonly used PSM type because of its simplicity, transparency to designers, and maturity of mask making techniques. The advantage of attenuated PSM is further enhanced when it is combined with off-axis illumination (OAI) and optical proximity correction (OPC). As has been known, OAI improves process latitude and enhances resolution for dense features, but is not as effective for isolated features. The philosophy of combining OAI and attPSM is to utilize the advantage of OAI for dense features and the advantage of attPSM for isolated features [1]. This combination results in better performance than attPSM or OAI used separately. Properly biasing and applying assist features to isolated features also improves the process window. However, the performance of isolated features with these combinations (PSM, OAI, and OPC) is still not as good as dense features.

It is well known that phase shift mask imaging is based on a destructive interference mechanism. The degree of interference depends on the degree of coherence of the illumination system. If the illumination is completely incoherent, then the image is the summation of intensity point spread functions from contributions of all points on the object. On the other hand, if the illumination is completely coherent, the amplitude (of the electrical field) point spread function is added from each point of the object, and the final intensity is the squared modulus of the summation of amplitudes [2]. For real lithographic systems, there is no complete coherence or incoherence. Theoretical analysis on the intermediate situation, i.e., partial coherence, can be found in Born and Wolf's classic book [3]. In their analysis, light is restricted to scalar fields and the polarization effect was not taken into account. In reality, light is a vector. The electric and magnetic fields vibrate in a plane perpendicular to the light propagation direction, called the polarization plane. This vector nature makes it necessary to include polarization effects if rigorous treatment is needed [4,5].

In order to have interference, electric fields have to vibrate in the same direction when polarization is taken into account. In photolithography tools, though the illumination light is unpolarized, polarization can still play an important role when two beams of light interact. Polarization mismatching (incomplete overlap of electric field directions) becomes worse as incident angles increase. No matter what kind of PSM is used, alternating, attenuated, or very high transmission attenuated, the degree of polarization matching determines the ultimate effectiveness of PSM when large angle components are involved. In this paper we use contact hole patterning as an example to demonstrate how partial coherence and polarization plays a role in imaging. PROLITH/3D simulation was used to understand these effects and to compare to experimental results.

Physical Background

Partial coherence theory is based on a complex cross-correlation function as described by Born and Wolf [3]. The cross correlation function $\Gamma_{12}(\mathbf{x_1}, \mathbf{x_2}, \tau)$ is expressed as

$$\Gamma_{12}(\mathbf{x_1}, \mathbf{x_2}, \tau) = \langle V_1(\mathbf{x_1}, t+\tau) * V_2^*(\mathbf{x_2}, t) \rangle \quad (1)$$

where V_1 is the optical disturbance at source point $\mathbf{x_1}$, and V_2 is the optical disturbance at source point $\mathbf{x_2}$; $\tau = t2 - t1 = \Delta L/c$; here τ is time difference between V_1 and V_2; ΔL is the optical path difference between V_1 and V_2, c is the light speed; and the brackets indicate a time average. When $\mathbf{x_1}$ and $\mathbf{x_2}$ merge together, then $\Gamma_{12}(\mathbf{x_1}, \mathbf{x_2}, \tau)$ becomes the self-coherence function, $\Gamma_{11}(\tau)$, representing the correlation at a fixed point in space at two different instants in time. This is called temporal coherence. When τ reduces to 0, $\Gamma_{12}(\mathbf{x_1}, \mathbf{x_2}, 0)$ becomes the mutual coherence function, representing correlation of two different points in space at the same time. This is called spatial coherence.

Temporal coherence arises primarily from considerations of the finite spectral width of light radiation and is characterized by the coherence length, L_{coh}, of the illumination.

$$L_{coh} = \lambda_0^2 / \pi\Delta\lambda \quad (2)$$

To reduce chromatic aberrations, DUV lithographic tools require a very narrow bandwidth. For example, $\Delta\lambda$ is about 0.6 pm for today's DUV steppers/scanners. From equation (2) it is easy to calculate that the coherence length for such a bandwidth illumination is on the order of a few centimeters, long enough to say those systems are temporally coherent from the perspective of the range of distances within the image plane under consideration.

Spatial coherence primarily arises from a consideration of the angular distribution of incident light due to an extended light source. The term "partial coherence" commonly used by industry is actually meant to describe a level of spatial coherence. In lithographic tools, a kind of Köhler illumination system is generally used. In Köhler illumination, all light beams from a given point on the source are essentially parallel as they leave the exit pupil of the illuminator (one plane wave for each source point). The mask, in turn, is placed at the exit pupil of the illumination system. Therefore, any point in the source can illuminate the whole mask with a constant, single incident angle. In other words, any given point on the mask is illuminated by all points in the light source. The partial coherence is defined as

$$s = \sin(\theta_{ill}) / NA_{lens} \quad (3)$$

The illuminator lens configuration controls the maximum incident angle of source illumination (θ_{ill}). The degree of spatial coherence is just this illumination angle range relative to the sine of the maximum acceptance angle of the objective lens (NA_{lens}). Light that emerges from a single source point, resulting in a single incident angle at

the mask, is spatially coherent. Light from different source points are assumed to have no spatial correlation to each other.

In the above treatment, a light disturbance was treated as a scalar function of time and position. However, light is actually a vector. Its electric and magnetic fields vibrate in a plane perpendicularly to the propagation direction. In order to have interference, besides the requirement of temporal and spatial coherence, a third condition, i.e., polarization matching, needs to be fulfilled. Polarization, or more precisely the vibration direction of the electrical field, has to be the same in order for two beams to interact. As shown in Figure 1, two light beams, even though both temporally and spatially coherent but polarized in different directions, do not completely overlap. Since only the overlapped portions of the electric fields will interfere, less than perfect overlap will result in less than optimal interference (and thus image quality).

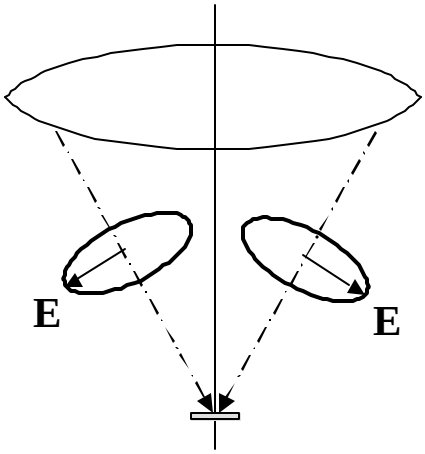

Figure 1. The polarization plane may not be perfectly overlapped when two interacting light beams have different incident angles. E is the electric field vector.

To illustrate how the polarization direction can affect image formation, consider the simple case of imaging 0.2 μm binary lines and spaces with 248nm wavelength, NA = 0.68, and coherent illumination. When the illumination is polarized along the length of the lines (Y-polarized, Fig. 2), the electric fields are completely overlapped when combining to form an image, resulting in maximum interference and image quality (Fig. 3). When the illumination is polarized across the feature width (X-polarized), there is significantly less overlap of the electric fields (similar to the picture in Fig. 1) and the image quality suffers. This effect is a function of angle. Figure 4 shows the same set of aerial image simulations for 0.3μm lines and spaces. The larger pitch produces diffraction orders that converge at the wafer at smaller angles. Thus, the X-polarized illumination case shows less deviation from the Y-polarized case for these larger features.

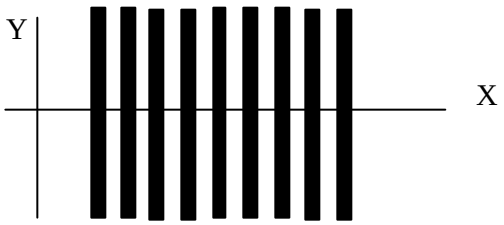

Figure 2. Geometry for the simulation of polarization effects on line and space features.

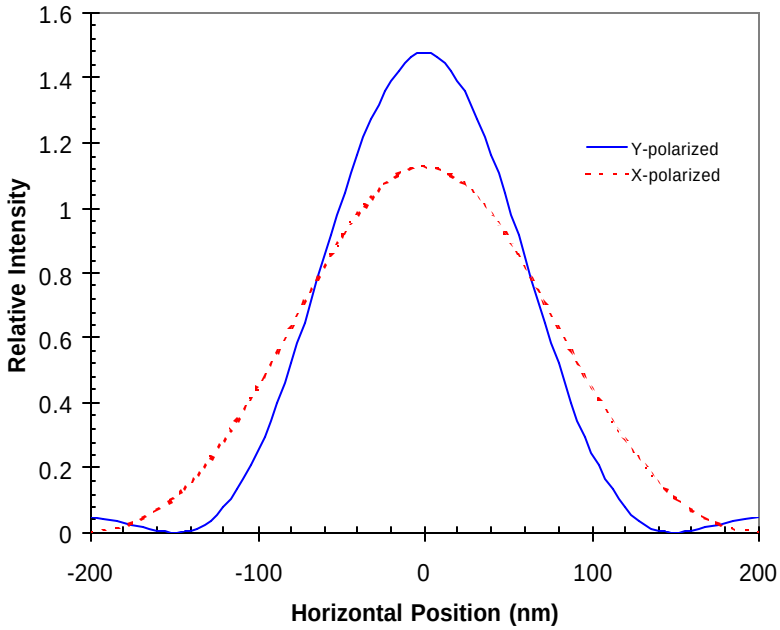

Figure 3. Aerial images of a 0.2µm space (0.4µm pitch) calculated for illumination polarizations along the length of the feature (Y-polarized) and across the width of the feature (X-polarized) with λ = 248nm, NA = 0.68, coherent illumination.

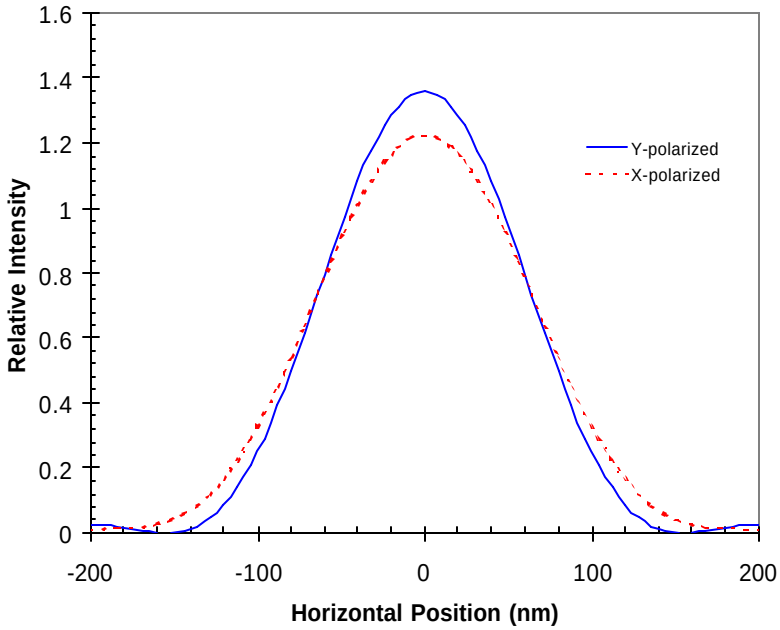

Figure 4. Aerial images of a 0.3µm space (0.6µm pitch) calculated for illumination polarizations along the length of the feature (Y-polarized) and across the width of the feature (X-polarized) with λ = 248nm, NA = 0.68, coherent illumination.

To explain the polarization effect further, a comparison between small sigma (Fig. 5a) and large sigma illumination (Fig. 5b) is shown. For easy understanding, the illumination light here is assumed to be linearly polarized in the plane of the picture. It is interesting to notice that light beams 2 and 4 maintain the same polarization direction from small sigma to large sigma illumination, since they are essentially *s*-polarized (vibration of the electric field is perpendicular to the principle plane). However, the polarization mismatch between light beams 1 and 3 increases when the illumination condition changes from small sigma to large sigma, since they are *p*-polarized (vibration of the electric field is parallel to the principle plane). From this example, we can see that the actual interference effect is very complicated when the vector nature of light is taken into consideration. Adding another complexity, the interaction angles change due to refraction when light beams enter the resist thin film. Detailed discussion on the thin film effect with polarization can be found elsewhere [4]. Though this change increases the polarization matching (due to the reduced interaction angle), the concept of overlapping electric fields stays the same. The polarization matching decreases as incident angle increases. A full vector treatment of partial coherence, called "partial polarization" can be found in references 6 and 7.

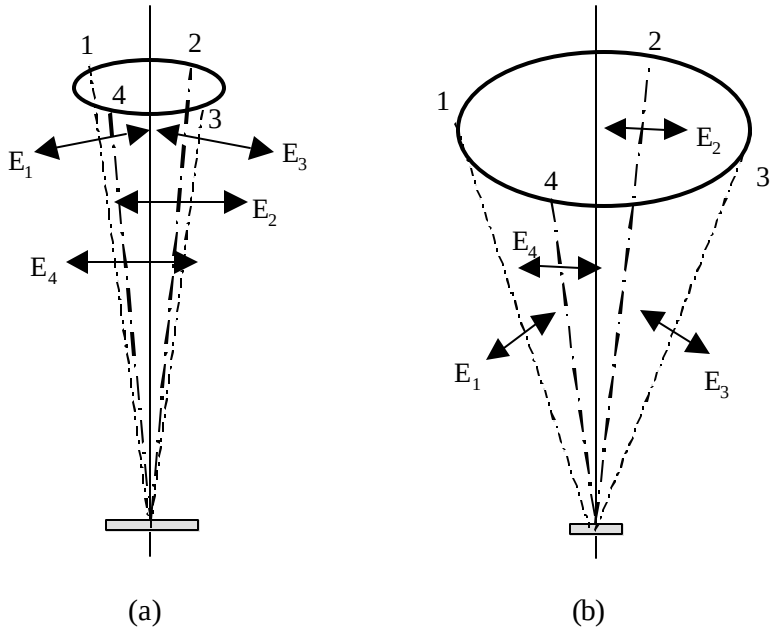

Figure 5. Schematics of how polarization can make an impact on the coherent interaction of light: (a) small incident angle illumination; (b) large incident angle illumination. The lines with double arrows indicate the polarization direction. E is the electrical field vector.

The impact of illumination source shape can be further illustrated through aerial image simulations. For example, for the 0.2 μm lines and spaces of Figure 3, if annular illumination is used instead of coherent illumination, the range of angles of the light actually converging to form the image is quite different. In this case, the difference between the two polarizations is much less for annular illumination than coherent illumination (Fig. 6).

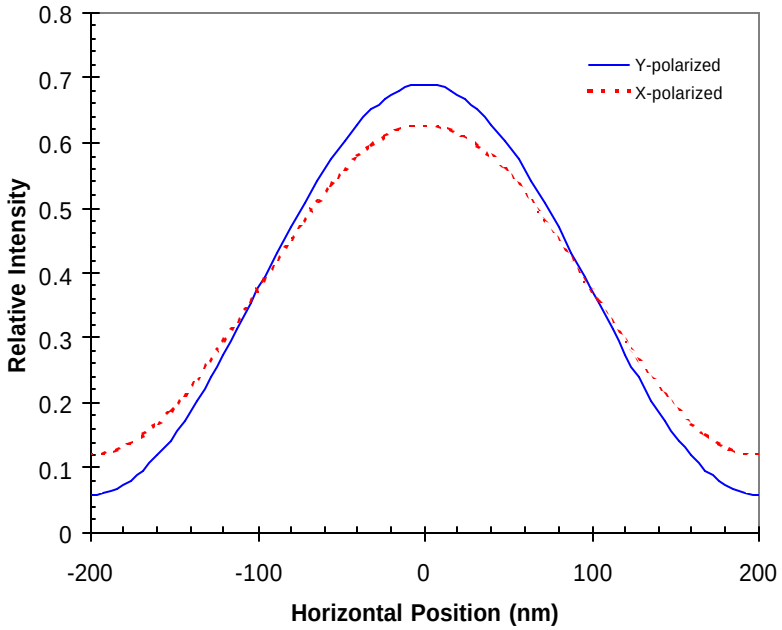

Figure 6. Aerial images of a 0.2μm space (0.4μm pitch) calculated for illumination polarizations along the length of the feature (Y-polarized) and across the width of the feature (X-polarized) with λ = 248nm, NA = 0.68, annular illumination (0.75/0.375).

The illumination light in an actual lithographic tool is either unpolarized or circularly polarized, since linear polarized light may cause orientation-dependent differences in the image formation process. However, the vibration direction of the electric field is still well defined in the polarization plane, which is perpendicular to the light travel direction. Unpolarized light can be thought of as the incoherent summation of two orthogonal polarization states. Therefore, polarization matching plays a role statistically for interfering beams, even with unpolarized illumination. Good matching occurs when the polarization planes of interfering beams have similar orientations.

Experiment and Results

Six oxide substrate wafers were exposed by a DUV scanner (λ = 248nm, numerical aperture = 0.68). Photoresist was coated on top of an organic BARC. Six different illumination modes were used to collect resist critical dimension (CD) data: conventional illumination with sigmas equal to 0.4, 0.5, 0.6, 0.66, and 0.75, and a 0.75/0.375 half-annular illumination configuration. An attenuated phase shift mask with 6% transmission was used. Focus-exposure data were collected for two different contact hole patterns: an array of 0.21 μm holes with 0.4 and 0.7 μm pitches. Exposure energy was adjusted to achieve the target resist CD of 0.21 μm for all six illumination modes.

CD (SEM top-down measurement) through focus curves for 0.4 um pitch (dense array) and 0.7 um pitch (semi-isolated array) contact holes are plotted in Fig. 7a and Fig. 7b, respectively. Comparing the two groups of curves, it is apparent that the depth of focus (DOF) increases as sigma increases for dense patterns, and vise versa for the semi-isolated patterns. Following the same trend, half-annular illumination gives the best perforce for dense patterns, but the worst performance for isolated patterns.

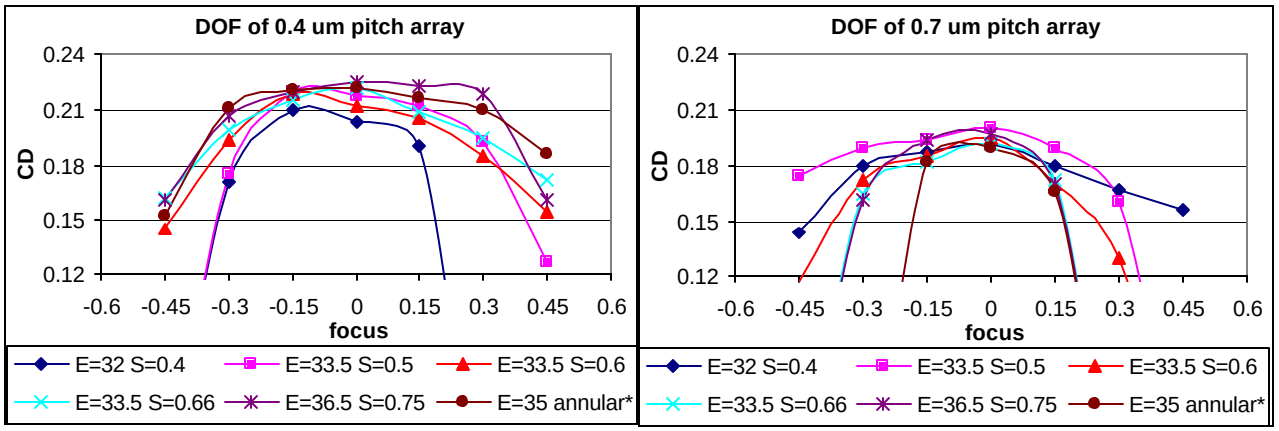

(a) (b)

Figure 7. Depth of focus of six different sigmas with the same lens NA. Exposures were adjusted to have similar resist CD target. (a) 0.4 um pitch array; (b) 0.7 um pitch array.

Fig. 8 shows top-down resist profiles for a small pattern area in which dense, semi-dense, and isolated features are included. In Fig. 8a, at s = 0.4, severe sidelobes were observed. It has been demonstrated that sidelobe printing strongly depends on the coherence factor [8]. In addition to the sidelobes, large pattern distortions due to residual lens aberrations were observed in the defocused condition, especially for the center hole in the geometrical center of a rectangular array, where four holes are placed in four corners. In Fig. 8b, s = 0.5, the sidelobe margin is improved significantly. The distortion of the center hole was still observed. In Fig. 8c and Fig. 8d, sigma equals 0.6 and 0.66, respectively, and pattern fidelity looks good from +0.3 μm to –0.3 μm focus. In Fig. 8e, s = 0.75, though pattern fidelity still looks OK for zero and positive focus, a small CD size for the isolated holes can be seen at –0.3 μm defocus. In Fig. 8f, which has half annular illumination, isolated holes are significantly smaller in the negative defocus condition and disappear in the positive defocus condition. However, dense holes still look good through focus.

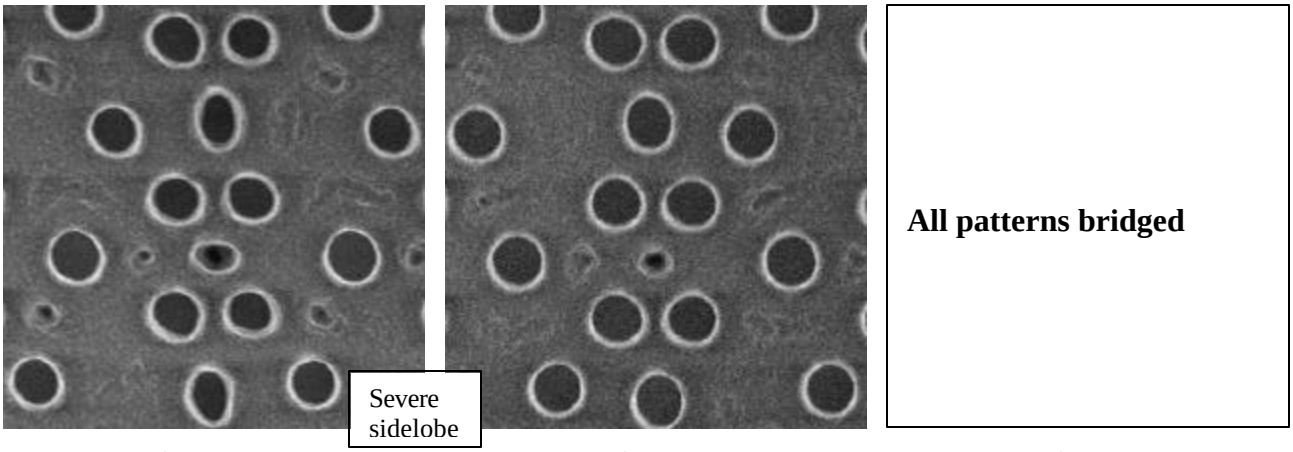

f = -0.3 f = 0 f = +0.3

(a) σ = 0.4

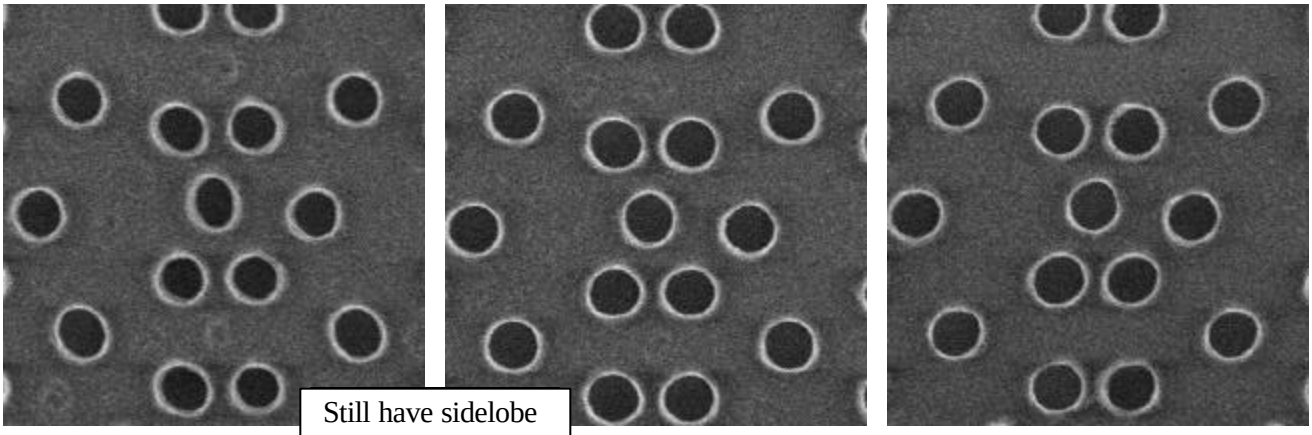

f = -0.3 f = 0 f = +0.3

(b) σ = 0.5

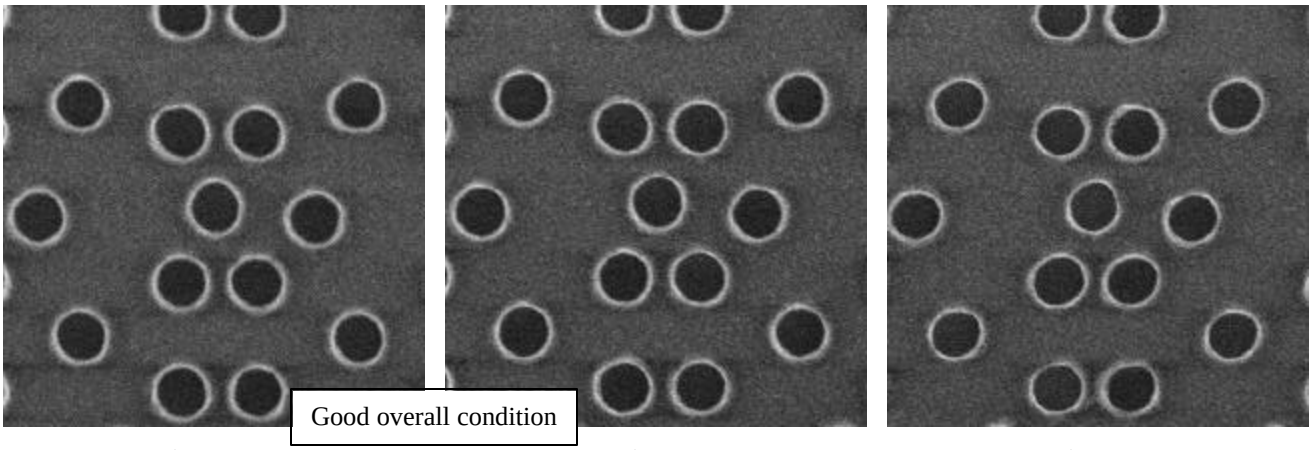

f = -0.3 f = 0 f = +0.3

(c) σ = 0.6

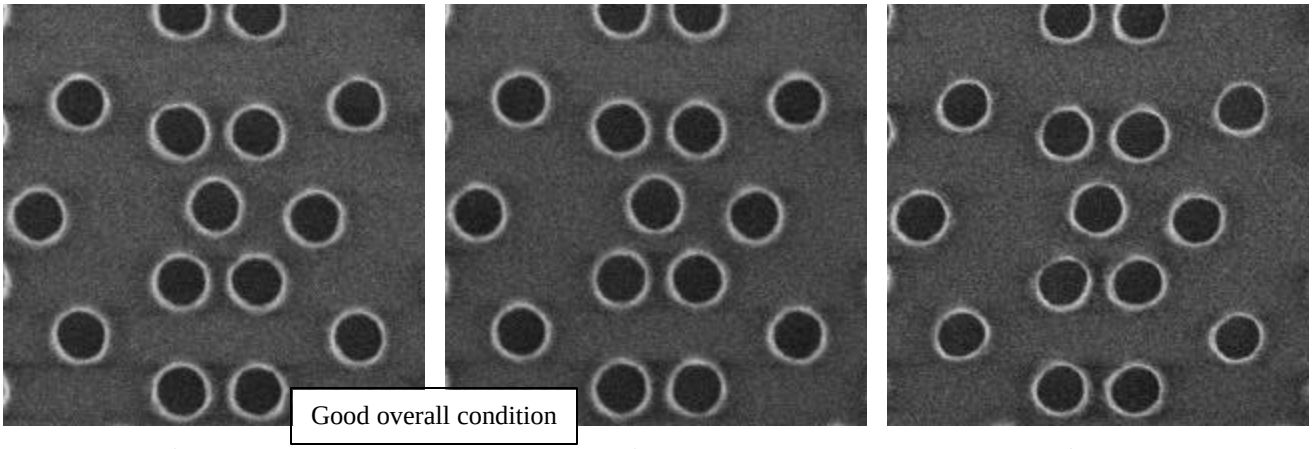

f = -0.3 f = 0 f = +0.3

(d) σ = 0.66

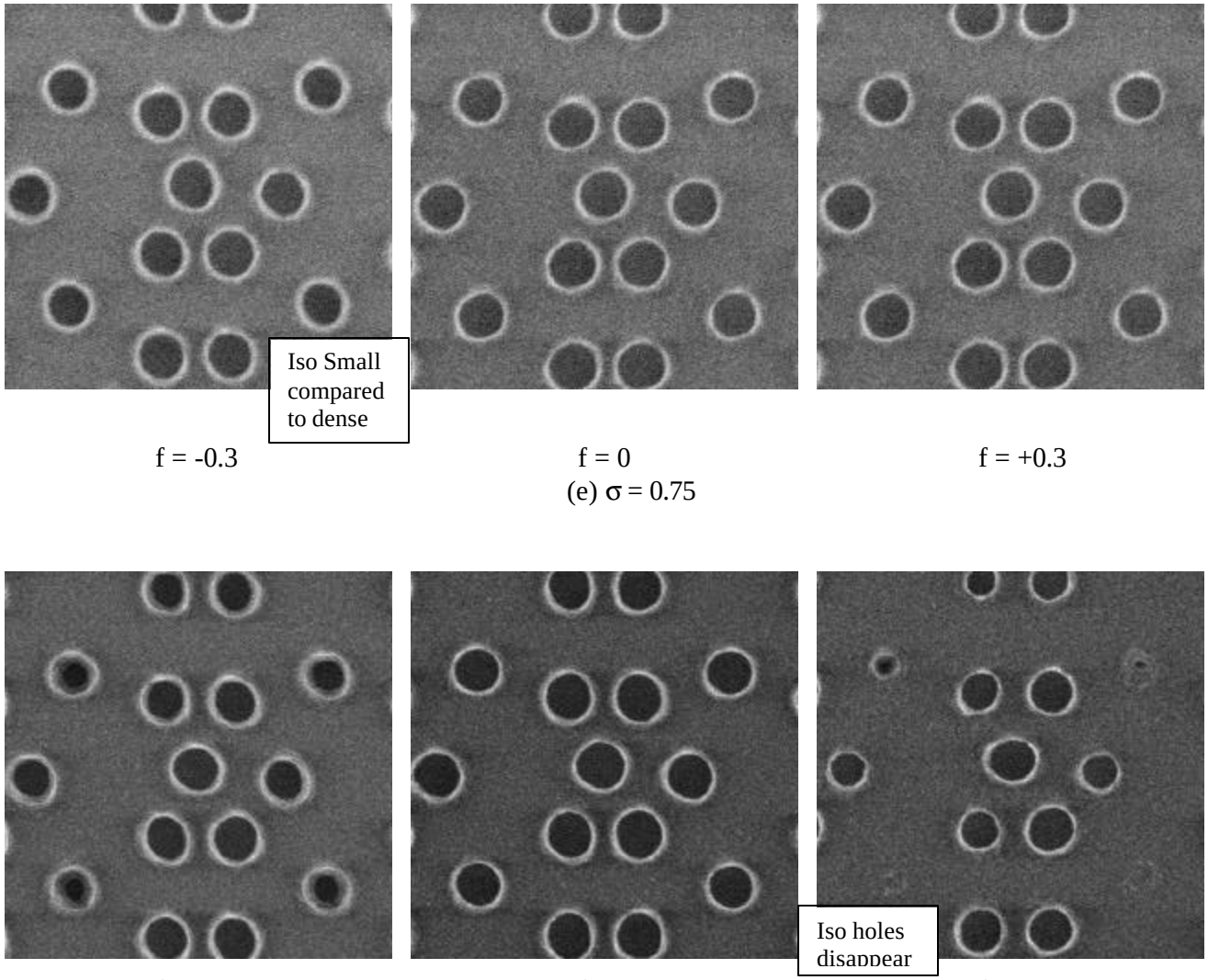

Figure 8. Top-Down SEM resist images for six sigmas with the same NA, at three different focus positions: (a) σ = 0.4; (b) σ = 0.5; (c) σ = 0.6; (d) σ = 0.66; (e) σ = 0.75; (f) σ = 0.75 / 0.375 half annular.

Both Fig. 7 and Fig. 8 show the best overall condition is medium sigma, around 0.6 to 0.66. Although small sigma gives the best DOF for isolated patterns, it causes sidelobe and distortion problems as seen in Fig. 8a. It is also not surprising that annular illumination is good for dense patterns since it collect more first order components than conventional illumination. The same argument is applied to large sigma illumination since it contains more off-axis components than small sigma illumination. However, isolated patterns with annular illumination are still not as good as with small sigma illumination. The limiting factor in annular illumination is still the isolated patterns even with phase shift reticles.

To further differentiate between possible polarization and partial coherence effects, simulations were performed in scalar mode, where the impact of polarization is ignored, as well as in full vector mode. Fig. 9 shows a comparison of scalar simulation to experiment for the in-focus 0.4 and 0.5 sigma cases from Fig. 8. As can be readily seen, both qualitative and quantitative agreement between simulation and experiment shows that

partial coherence has a strong influence on the printing of sidelobes. Vector simulations did not give appreciably different results, indicating that at this NA, the polarization effects discussed above are still small.

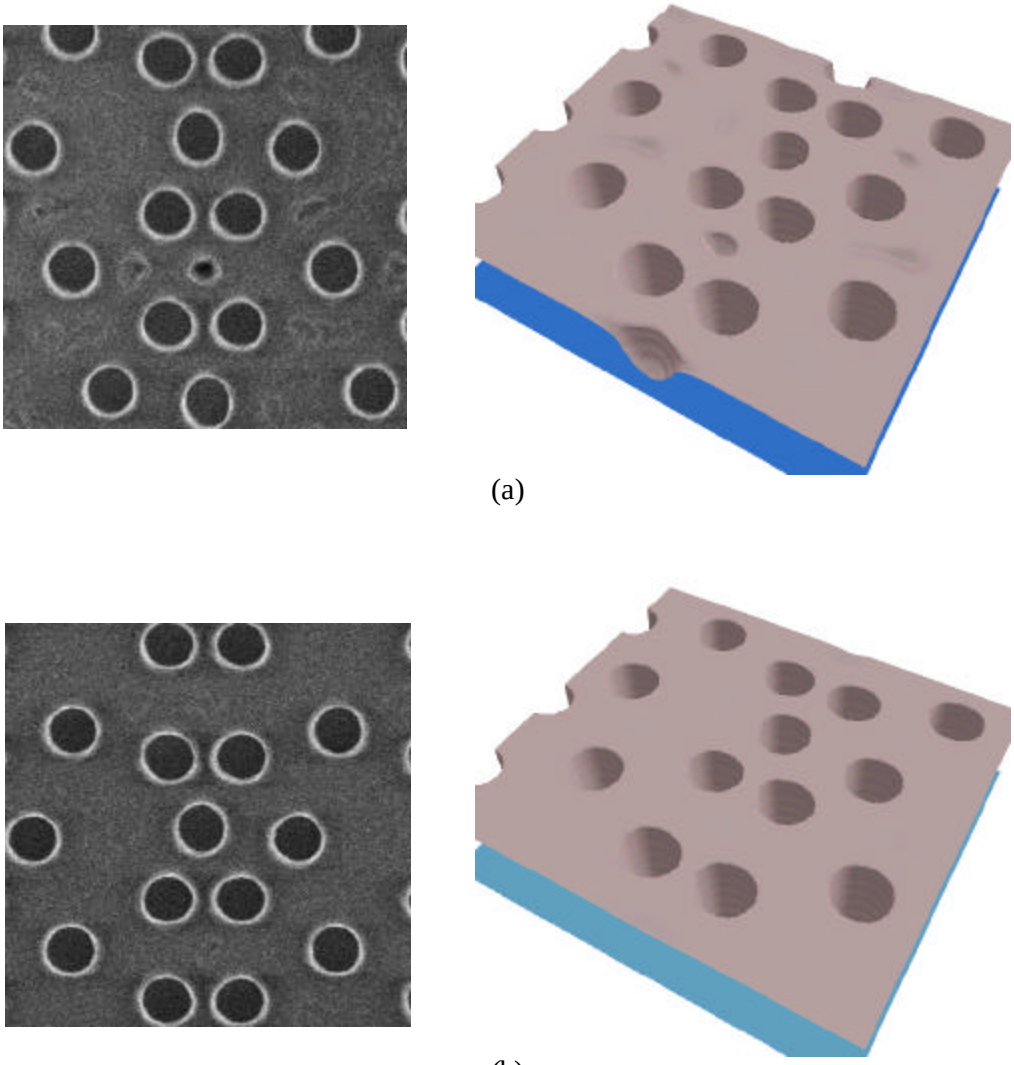

Figure 9. Comparison of PROLITH/3D simulations to experiment for (a) $\sigma = 0.4$, and (b) $\sigma = 0.5$ clearly show that partial coherence has a dominant affect in sidelobe printing.

Conclusion

As discussed above, polarization can play a role in applying PSM, depending on the conditions. In order to have phase shift working properly, good polarization matching is needed. Partial coherence, with its effect on the incident angle illumination, can impact how polarization influences image formation. When attPSM is combined with OAI, dense features are further enhanced by off-axis illumination. However, as OAI is not effective for isolated features, the limiting factor in this combination is isolated features. Although polarization seems to play only a minor role at the 0.68 numerical aperture used in this study, at higher NAs the effects will

be significant. Carefully balancing of the polarization requirement in the illumination condition should further improve the performance of attPSM plus OAI at very high numerical apertures.

Acknowledgments

The authors would like to thank Maureen Hanratty, Mark Terry, and Simon Chang of Texas Instruments for many useful discussions. The author is also grateful to Francis Celii of Texas Instruments for his help in extracting film stack information from Variable Angle Spectroscopic Ellipsometry.

References

1. T. A. Brunner, "Rim phase-shift mask combined with off-axis illumination: a path to 0.5λ/NA geometries", *Proc. SPIE*, Vol. 1927 (1993) p. 54.
2. J. W. Goodman, Introduction to Fourier Optics, McGraw-Hill, (New York: 1968).
3. M. Born and E. Wolf, Principle of Optics, Pergamon Press, (New York: 1964).
4. D. G. Flagello, T. Milster, and A. E. Rosenbluth, "Theory of High-NA Imaging in Homogeneous Thin Films," *Journal Optical Society of America*, Vol. 13, No. 1 (Jan. 1996) pp. 53-64.
5. S. Asai, I. Hanyu, and M. Takikawa, "Resolution Limit for Optical Lithography Using Polarized Light Illumination," *Japanese Journal of Applied Physics*, Vol. 32, Pt. 1, No. 12B (1993) pp. 5863-5866.
6. E. L. O'Neil, Introduction to Statistical Optics, Addison-Wesley Publishing, (Reading, Mass.: 1963).
7. M. J. Beran and G. B. Parrent, Jr., Theory of Partial Coherence, Prentice Hall, (Englewood Cliffs, N. J.: 1964).
8. Z. Mark Ma and Andrew Anderson, "Preventing sidelobe printing in applying attenuated phase shift reticles", *Proc. SPIE*, Vol. 3334 (1998).